Int J Biochem Mol Biol 2011;2(4):328-339
www.ijbmb.org /ISSN:2152-4114/IJBMB1110003

Original Article

Structural evidence for the order of preference of inorganic substrates in mammalian heme peroxidases: crystal structure of the complex of lactoperoxidase with four inorganic substrates, SCN^-, I^-, Br^- and Cl^-

Amit K Singh, Nisha Pandey, Mau Sinha, Punit Kaur, Sujata Sharma, Tej P Singh

Department of Biophysics, All India Institute of Medical Sciences, New Delhi, India

Received October 18, 2011; accepted November 12, 2011; Epub November 20, 2011; Published December 15, 2011

Abstract: Lactoperoxidase (LPO) is a member of the family of mammalian heme peroxidases. It catalyzes the oxidation of halides and pseudohalides in presence of hydrogen peroxide. LPO has been co-crystallized with inorganic substrates, SCN^-, I^-, Br^- and Cl^-. The structure determination of the complex of LPO with above four substrates showed that all of them occupied distinct positions in the substrate binding site on the distal heme side. The bound substrate ions were separated from each other by one or more water molecules. The heme iron is coordinated to His-351 $N^{\varepsilon 2}$ on the proximal side while it is coordinated to conserved water molecule W-1 on the distal heme side. W-1 is hydrogen bonded to Br^- ion which is followed by Cl^- ion with a hydrogen bonded water molecule W-5′ between them. Next to Cl^- ion is a hydrogen bonded water molecule W-7′ which in turn is hydrogen bonded to W-8′ and N atom of SCN^-. W-8′ is hydrogen bonded to W-9′ which is hydrogen bonded to I^-. SCN^- ion also interacts directly with Asn-230 and through water molecules with Ser-235 and Phe-254. Therefore, according to the locations of four substrate anions, the order of preference for binding to lactoperoxidase is observed as $Br^- > Cl^- > SCN^- > I^-$. The positions of anions are further defined in terms of subsites where Br^- is located in subsite 1, Cl^- in subsite 2, SCN^- in subsite 3 and I^- in subsite 4.

Keywords: Antimicrobial activity, heme, oxidation, peroxidase, crystal structure, complex, halide ions

Introduction

The family of four mammalian peroxidases with a covalently linked heme moiety includes lactoperoxidase (LPO), myeloperoxidase (MPO), eosinophil peroxidase (EPO) and thyroid peroxidase (TPO). These enzymes catalyze the H_2O_2-dependent oxidation of a variety of substrates such as halides (I^-, Br^- and Cl^-), pseudohalides (SCN^-) and organic substrates which include phenols [1, 2], catecholamines and catechols [3-5] as well as other experimental model compounds such as aromatic amines [6], polychlorinated biphenyls [7], steroid hormones [8-10] and polycyclic aromatic hydrocarbons [11]. So far, structural studies have been carried out successfully on MPO and a few of its complexes [12-15] and LPO and its several complexes [16-21]. However, there is still an ambiguity about the relative preferences of these heme peroxidases for various inorganic substrates [22-25]. In this context, binding studies have indicated that MPO follows a preference [23] in the order of $Cl^- > Br^- > SCN^- > I^-$; EPO's preference [24] is shown as $Br^- > SCN^- > I^-$ while LPO has been shown to prefer [22] in the order of $SCN^- > I^-$ and TPO also prefers [25] the order as $SCN^- > I^-$. The information about the preference for Cl^- and Br^- by LPO is not available. The structures of bound single inorganic substrates with MPO [14-15] and LPO [16, 18] are known. We report here the structure of a complex of LPO with four anionic substrates, Cl^-, Br^-, SCN^- and I^-. In this case LPO was crystallized in the presence of equimolar concentrations of four inorganic substrates, Cl^-, Br^-, SCN^- and I^-. The structure determination revealed a new information about the presence of four bound anionic inorganic substrates and the positions they occupied in the substrate-diffusion channel on the distal heme

side. This is an important observation showing the preferred positions of Cl^-, Br^-, SCN^- and I^- in the binding site when all the four anions had identical opportunities for binding. The position of ions, SCN^-, I^-, Br^-, and Cl^- are clearly separated from each by one or more water molecules between them. The observed positions of anions with respect to the heme iron in LPO suggest that the order of preference could be as Br^-, Cl^-, SCN^- and I^- with Br^- as the most preferred and I^- being the least in that order. This is the first structural evidence showing a clear preference by LPO for anionic substrates. Based on this work, the binding region on the distal heme side has been subdivided into four sub-regions called as S1, S2, S3 and S4 as subsites in the substrate binding site of LPO.

Materials and methods

Protein purification

Fresh bovine milk was collected from Indian Veterinary Research Institute, Izatnagar, India. The samples were skimmed and separated from fat. These were diluted twice with 50 mM Tris-HCl (pH 7.8). Cation exchanger CM-Sephadex C-50 (7gl^{-1}) equilibrated in 50 mM Tris-HCl, pH 7.8 was added by stirring slowly for about one hour with mechanical stirrer. The gel was allowed to settle and the solution was decanted. In order to remove the unbound proteins, the protein bound gel was washed with an excess of 50 mM Tris-HCl (pH 8.0). The washed gel was loaded on a CM-Sephadex C-50 (Pharmacia, Uppsala, Sweden) column (100 × 2.5 cm) and equilibrated with 50mM Tris-HCl, pH 8.0. The elution of LPO was carried out with a linear gradient of 0.0 - 0.5 M NaCl using same above buffer. The protein fractions with Rz value of 0.8 and above were pooled and concentrated using an Amicon ultra filtration cell (Millipore, Billerica, MA, USA). The concentrated protein sample was passed through a Sephadex G-100 column (100 × 2cm) using 50 mM Tris-HCl buffer, pH 8.0. The elution was done at a flow rate of 6.0 ml/hr. The fractions of Rz value of 0.9 and above were pooled and dialyzed against deionized water. The lyophilized samples were stored at 253 K for further analysis.

LPO activity measurements

The activity assay was carried out following the procedure of Shindler and Bardsley [26] with some modifications to suit certain requirements. The 3.0 ml of 1 mM 2,2-azinobis(3-ethylbenzthiazolinesulfonic acid) (ABTS) in 0.1 M phosphate buffer, pH 6.0, was mixed with 0.1 ml of sample in 0.1 M phosphate buffer, pH 7.0, containing 0.1% gelatin to initialize the spectrophotometer (PerkinElmer Life Sciences, Waltham, Massachusetts, USA). The 3.0 ml of 1 mM ABTS solution was mixed with 0.1 ml of protein sample and 0.1 ml of 3.2 mM hydrogen peroxide solution. The absorbance was measured at 412 nm as a function of time for 2 to 3 min. The rate of change of absorbance was constant for at least 2 min. The one unit of activity is defined as the amount of enzyme catalyzing the oxidation of 1 μmol of ABTS min^{-1} at 293 K (molar absorption coefficient 32,400 M^{-1} cm^{-1}). The activity of LPO was found to be 5.3 units ml^{-1}. The purity of LPO was also determined by absorbance ratio A_{412}/A_{280} (RZ value). The RZ value for the purified LPO was found to be 0.932.

Crystallization of LPO with halides and pseudo-halide

The purified samples of protein were dissolved in 0.05 M tris-HCl buffer (pH 8.0), to a concentration of 50 mg/ml. The mixture of halides (I^-, Br^- and Cl^-) and thiocyanate (SCN^-) was prepared using equal molar amounts at an overall concentration of 100 mg/ml. It was added to the protein solution in 1:1 ratio (v/v). Separately, a solution with 0.2 M ammonium acetate and 20% (w/v) PEG-3350 was prepared for the crystallization reservoir. The 6 μl of protein-ligand solution was mixed with 6 μl of reservoir solution to prepare 12 μl drops for hanging drop vapour diffusion method using 24-well Limbro plates. The rectangular-shaped and dark brown colored crystals measuring up to 0.4 × 0.4 × 0.3 mm^3 were obtained after one week. These crystals were also soaked in the solution containing equimolar amounts of SCN^-, I^-, Br^-,and Cl^- ions for more than 48 hours.

X-ray intensity data collection and processing

Using these crystals, the X-ray intensity data were collected at the DBT-sponsored Synchrotron beamline BM-14 of the European Synchrotron Radiation Facility (ESRF) in Grenoble (France) on a MAR CCD detector (MAR, USA Inc. Evanston Il). In order to minimize the radiation damage, crystals were placed in nylon loops

Table 1. Data collection and refinement statistics

Data collection	
Space group	$P2_1$
Unit cell dimensions (Å)	a = 54.2, b = 79.8, c = 77.5
β (°)	102.6
Number of molecules in the unit cell	2
Vm (Å3/Da)	2.5
Solvent content (%)	50.0
Resolution range (Å)	75.66 – 1.77 (1.80-1.77)
Total number of measured reflections	120,995
Number of unique reflections	62,590
Completeness of data (%)	98.9 (96.0)
$*R_{sym}$ (%)	6.1 (42.3)
I/s(I)	39.1 (2.9)
Refinement	
$*R_{cryst}$ (%)	19.0
R_{free} (%) (5% data)	23.6
Protein atoms	4770
Calcium ion	1
Heme (1)	43
Water oxygen atoms	763
NAG atoms (8 NAG + 2 MAN residues)	134
Diethylene glycol (1) atoms	7
Monoethylene glycol (1) atoms	4
Thiocyanate (1) atoms	3
Iodide	15
Bromide	1
Chloride	1
Zinc	1
Glycerol (3 molecules) atoms	15
2-methyl-2,4-pentanediol (1 molecule) atoms	8
R.m.s.d. in bond lengths (Å)	0.02
R.m.s.d. in bond angles (°)	2.0
R.m.s.d. in dihedral angles (°)	13.8
Overall G factor	-0.06
Average B–factor ($Å^2$)	
Wilson Plot	23.9
Main chain atoms	28.0
Side chains and water molecules	33.6
Overall	31.3
Ramachandran's plot	
Residues in the most favored regions (%)	89.5
Residues in the additionally allowed regions (%)	10.5
PDB Code	3NYH

The values in parentheses correspond to the values in the highest resolution shell; $*R_{sym} = \sum_{hkl}\sum_i |I_i(hkl) - \langle I(hkl)\rangle| / \sum_{hkl}\sum_i I_i(hkl)$; $*R_{cryst} = å_{hkl} \div F_o(hkl) - F_c(hkl) \div / å_{hkl} \div F_o(hkl) \div$ where F_o and F_c are observed and calculated structure factors, respectively.

and kept at 100K in a nitrogen stream during the measurements. The water ice formation was avoided by pre-incubation of the crystals for 3 minutes in the reservoir solution containing 22% w/v PEG-3350. A complete data sets was collected using one crystal. The data were processed and scaled with DENZO and SCALEPACK from the HKL-2000 package [27]. The crystals belong to monoclinic space group $P2_1$ with one molecule in the asymmetric unit. The results of data collection and processing statistics are given in **Table 1**.

Structure determination and refinement

The structure was determined with molecular replacement method using the coordinates of native lactoperoxidase as a model (PDB ID: 3GC1). The rotation and translation functions and rigid body refinements performed using the

data between 12.0 and 4.0 Å yielded a clear solution with correlation coefficient of 64% and an R factor of 35.7%. The refinement was carried out using program CNS [28]. The (|2Fo - Fc|) and (|Fo - Fc|) maps were calculated to adjust the protein molecule in the electron density using the program O [29]. Several cycles of restrained positional refinement with individual B-factors and several rounds of simulated annealing from 3000 to 300 K allowed the correct tracing of the flexible loops where conformations were markedly different from the initial model. The manual chain tracing was carried out using omit maps across the entire protein molecule as the refinement progressed. At the end of this stage, the R_{cryst} and R_{free} factors dropped to 0.26 and 0.29 respectively. The Fourier (|2Fo - Fc|) and difference Fourier (|Fo - Fc|) maps computed at this stage showed three spherical electron densities with considerable differences in peak heights as well as one elongated electron density in the substrate-binding channel on the distal heme side (**Figure 1A**). According to clearly calibrated peak heights in the difference (|Fo - Fc|) electron density map, the specific halide ions, I^-, Cl^- and Br^- were modeled. In order to further confirm the correctness of the identification of halides, their positions were interchanged and refined. The refinements were followed by examining the variations in B-factors. The occupancies of all the three halides were kept constant at 1.0. On interchanging halide atoms with one another the B-factors either increased or decreased drastically indicating inaccuracy in the selection of halide ions. In order to identify the correct nature of halide atoms the occupancies were also varied to adjust the higher and lower peak electron densities. These calculations showed inconsistencies and the best refinement values were observed when Br^- occupied the nearest position to the conserved water molecule W-1 while I^- was placed at the most distant position. The iodide ion has been observed at the assigned position in other structures as well when only iodide anion was used specifically (PDB IDs: 3QL6 and 3PY4). The Cl^- ion showed the best agreement at the middle position. The positions of Br^- and Cl^- ions were interchanged and several variations in occupancies and B-factors were calculated. However, the best fit with optimum B-factors and occupancies gave a clear indication of their respective positions as assigned here (**Figure 1**). The final average value of B-factor for the well defined backbone atoms of the protein is 28Å^2. The well coordinated heme iron has a B -factor of 17Å^2. The B-factors for Br^-, Cl^-, I^- and S of SCN^- are 28Å^2, 27Å^2, 43Å^2 and 35Å^2 respectively while the average value for water oxygen atoms is 33Å^2. Since the protein was co-crystallized with halide and thiocyanate ions and since halides were only single atoms, it was expected that they will occupy respective positions with full occupancies. Additionally the crystals were further soaked in the solution containing halides and thiocyanate ions to make it doubly sure that their occupancies were full. Therefore, the identification of halide atoms appears to be reasonably accurate. In addition to these spherical shaped electron densities in the channel an asymmetrical dumble-shaped electron density was also observed into which, SCN^- ion was modeled nicely. Previously also SCN^- ion has been observed at this position (PDB IDs: 3QL6, 3Q9K, 3PY4 and 3OGW). There were other spherical shaped densities on the distal heme side at lower sigma cutoffs between the positions of halide ions into which water molecules were modeled and assigned as W-1, W-3′, W-5′, W-6′, W-7′, W-8′, W-9′, W-10′ and W-11′. These electron densities in the difference Fourier (|Fo - Fc|) map were further evaluated at various higher values of sigma cutoffs for ascertaining the correctness of halide ions. In the electron density map at 5δ cut off the densities for water atoms disappeared and the remaining densities confirmed the positions of S, Cl^-, Br^-, I^- and Ca^{2+} (**Figure 1B**). In the next step, the electron density was examined at 8δ cut off which distinguished the ions of I^- and Br^- from Cl^-, Ca^{2+} and S atom of SCN^- clearly (**Figure 1C**). The next calculation was made at 11δ cut off which confirmed the position of I^- and Br^- (**Figure 1D**). The final calculation at 14δ cut off showed the position of I^- only (**Figure 1E**). On having ascertained the correctness of halide atoms these were included in the subsequent cycles of refinement which were combined with several rounds of positional and restrained individual B-factor refinement steps. The additional non-protein electron densities observed above 3δ in (|Fo - Fc|) and 1.5δ in (|2Fo - Fc|) maps were interpreted as a heme moiety, ten carbohydrate residues from four glycan chains and one zinc ion. These and subsequent maps were also used for determining the positions of 763 water oxygen atoms by applying the usual criteria of hydrogen bonding with protein atoms or with other water molecules and also by qualifying them with optimum values of B factors at approximately 60Å^2.

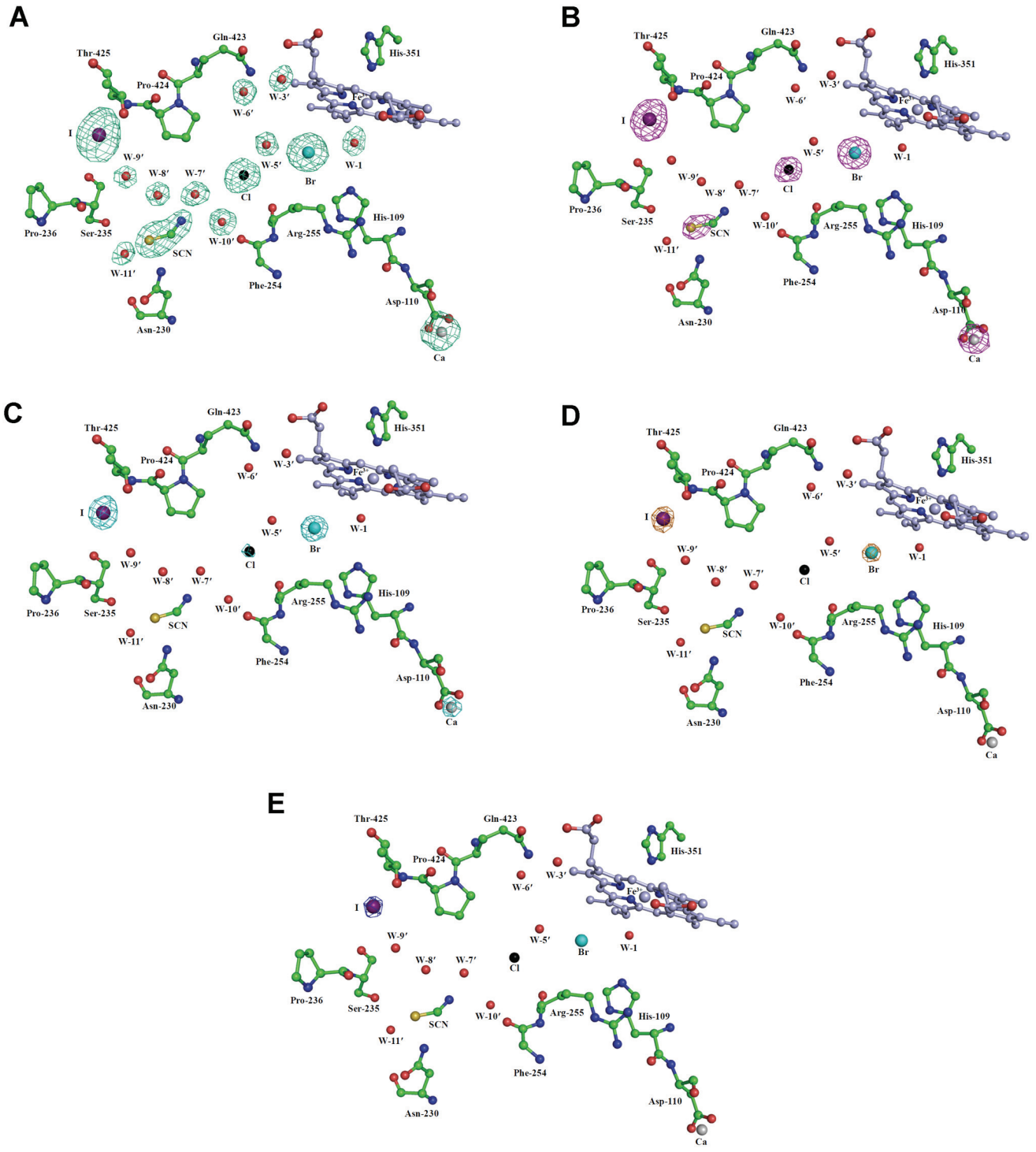

Figure 1. (A) The initial difference (|Fo - Fc|) Fourier map showing the electron densities at 3s cut off for I^-, W-11′(W-925) W-10′ (W-1166), W-9′ (W-1186), W-8′(W-1123), SCN^-, W-7′ (W-1134), Cl^-, W-6′ (W-719), W-5′ (W-1150), W-3′ (W-1136), Br^-, W-1 (W-790) and calcium ion. Figure was drawn using Pymol [33]. (B) The final Fourier (|2Fo - Fc|) map showing electron densities for I^-, Br^-, Cl^-, S atom of SCN^- and Ca^{2+} atoms at 5s cut off. (C) The final Fourier (|2Fo - Fc|) map showing electron densities for I^-, Br^-, Ca^{2+} and Cl^- ions at 8s cut off. (D) The final Fourier (|2Fo - Fc|) map showing electron densities for I^- and Br^- ions at 11s cut off. (E) The final Fourier (|2Fo - Fc|) map showing electron density for I^- ion at 14s cut off.

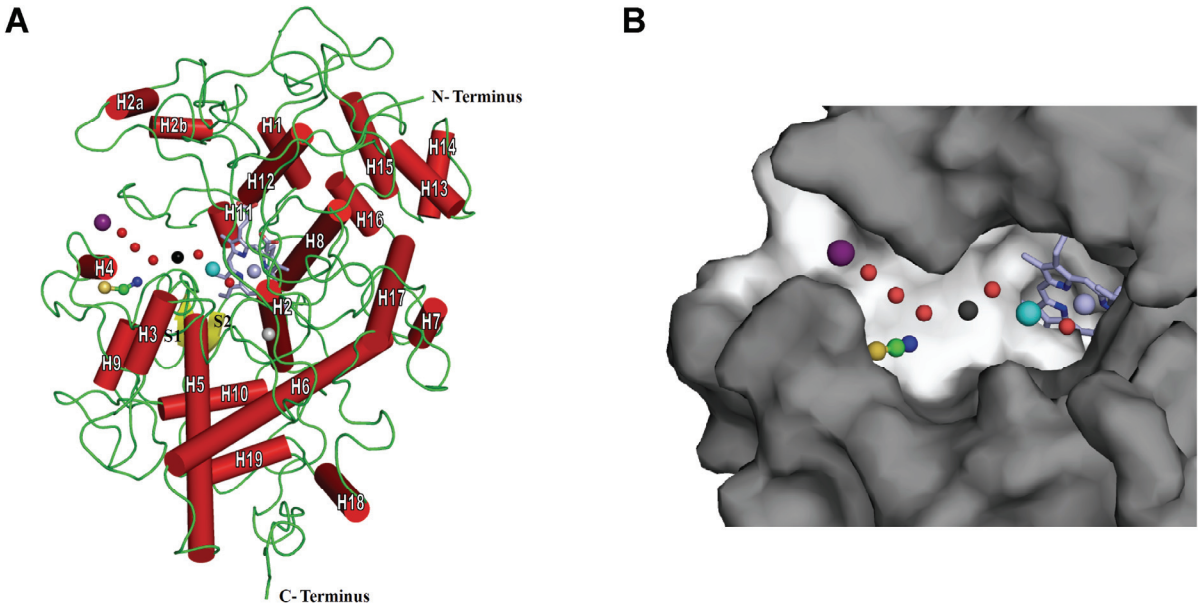

Figure 2. (A) The overall folding of the polypeptide chain of lactoperoxidase. The helices as cylinders (red) and β-strands as arrows (yellow) have been indicated and numbered. The heme moiety (blue) and substrate anions I^- (purple), SCN^- (yellow-green-blue), Cl^- (black), Br^- (cyan) while W-1, W-5′, W-7′, W-8′, W-9′, W-10′ and W-11′ are shown as red spheres. Ca^{2+} ion is shown in green. (B) The Grasp drawing for the regions around the substrate-binding cleft filled with heme moiety (light blue with iron in orange), Br^- (cyan), Cl^- (black), I^- (purple), SCN^- (yellow-green-blue) and water molecules in red.

After the final rounds of calculations with 3000 K simulated annealing coupled with positional refinement and restrained individual B-factor refinements, the R_{cryst} and R_{free} factors converged to 0.190 and 0.236 respectively. The refined coordinates of the lactoperoxidase complexed with halides, I^-, Br^-, Cl^- and SCN^- have been deposited in the Protein Data Bank (PDB ID: 3NYH). The statistics of data collection and refinement are listed in **Table 1**.

Results and discussion

Quality of the model

The final model as summarized in **Table 1** represents a well defined molecule of LPO that consists of residues from 1 to 595, a prosthetic heme group, 4 glycan chains and 763 water oxygen atoms. Four substrate ions, I^-, SCN^-, Cl^- and Br^- were observed in the substrate-binding channel on the distal heme side. Overall mean B-factor for all atoms is 31.3Å^2. The geometry of the protein molecule is close to ideal values with root-mean-square (r.m.s) deviations of 0.02Å and 2.0° from the standard values for bond lengths and angles respectively. The quality of the model as checked using PROCHECK [30] showed 89.5% of the non-Gly and non-Pro residues in the most favored regions of the Ramachandran plot [31]. The MolProbity score [32] was estimated to be at 75 percentile. The Ramachandran outliers were 0.51%, Cβ deviations >0.25Å were 0 while residues with bad angles were 0.17%. All other values were within the prescribed limits.

Overall structure

Overall structural organization of lactoperoxidase with four bound inorganic substrate ions in the diffusion channel is shown in **Figure 2A**. The protein adopts largely an α-helical fold consisting of 21 α-helices, H1 (residues, 75-83), H2 (residues, 98-111), H2a (residues, 123-132), H2b (residues, 149-152), H3 (residues, 197-203), H4 (residues, 236-240), H5 (residues, 260-283), H6 (residues, 289-317), H7 (residues, 319-325), H8 (residues, 341-353), H9 (residues, 383-389), H10 (residues, 391-399), H11 (residues, 415-420), H12 (residues, 433-444), H13 (residues, 449-495), H14

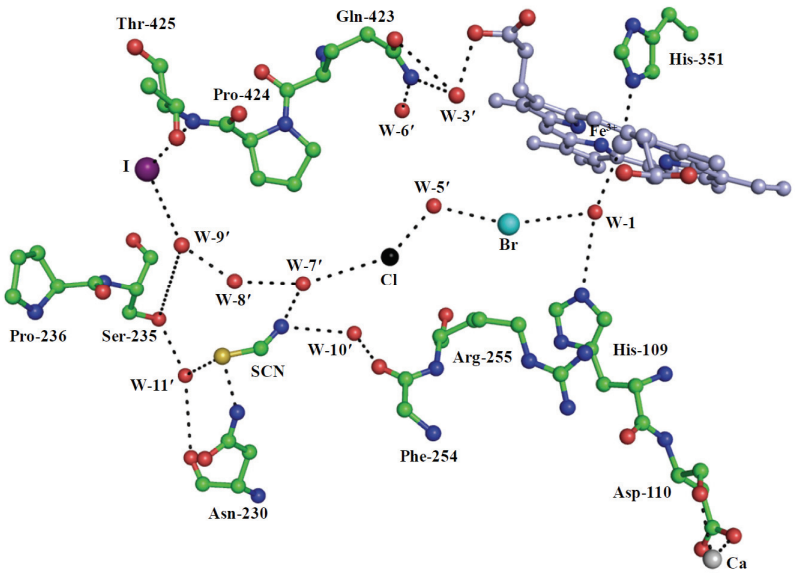

Figure 3. The hydrogen bonded interactions involving Br^-, Cl^-, I^-, SCN^-, Fe^{3+}, W-1 (E27), W-3¢ (E373), W-5¢ (E387), W-6¢ (E719), W-7¢ (E371), W-8¢ (E360), W-9¢ (E423), W-10¢ (E403) and W-11¢ (E162). The names in the parentheses correspond to the names in the PDB file: 3NYH. The coordinate linkages of Ca^{2+} ion are also shown.

(residues, 464-471), H15 (residues, 474-483), H16 (residues, 492-498), H17 (residues, 509-525), H18 (residues, 538-545), H19 (residues, 549-556). There are two short β-strands, S1 (residues, 357-359) and S2 (residues, 373-375). The helices H2a and H2b are absent in the structure of MPO (12). The elongated molecule of LPO with α-helices stacked one above the other is shown in **Figure 2A**, in which the heme moiety is sandwiched between α-helices, H2 on one side while H11 and H12 are on the opposite side. In addition to two covalent bonds between the heme moiety and the protein molecule, the heme group is very tightly packed. The heme iron forms a coordination bond with proximal His-351 $N^{\varepsilon 2}$ at distance of 2.2Å, while carboxylic group of one of the heme propionates forms ionic interactions with guanidinium groups of Arg-348 (2.8Å) and Arg-440 (2.7Å) of α-helices H8 and H12 respectively. The carboxylic group of the second propionate moiety forms a hydrogen bond (2.9Å) with Ala-114 N of helix H2. On the distal side, His-109 interacts with heme iron through conserved water molecule, W-1. A deep channel is formed on the distal heme side with well defined boundaries. The channel connects the deeply buried heme moiety to the surface of protein molecule (**Figure 2B**). The walls of the channel consists of a flexible loop, Lys-420 - Leu-433 on one side while the segments, Gln-105 - Phe-113, Asn-231 - Thr -243, Gly-252 - Ile-260 and Leu-374 - Asn-382, make the remaining walls of the channel. It is pertinent to note here that the internal character of the substrate-diffusion channel is predominantly hydrophobic in nature. The conformation of one of the loops, Gln-105 – Phe-113 is stabilized by the calcium ion which forms a regular pentagonal bipyramidal coordination polyhedron in which the calcium ion is coordinated with seven oxygen atoms in the structure, Ca^{2+} • • • Asp-110 $O^{\delta 1}$ = 2.4Å, Ca^{2+} • • • Asp-110 O = 2.2Å, Ca^{2+} • • • Thr-184 $O^{\gamma 1}$ = 2.4Å, Ca^{2+} • • • Asp-110 O = 2.3Å, Ca^{2+} • • • Phe-186 O = 2.3Å, Ca^{2+} • • • Asp-188 $O^{\delta 1}$ = 2.4Å and Ca^{2+} • • • Ser-190 O^{γ} = 2.4Å.

Bindings of SCN^-, I^-, Cl^- and Br^-

The four inorganic substrate ions have been observed in the substrate diffusion channel on the distal heme side. As seen from **Figure 3**, the heme iron is coordinated to proximal His-351 (Fe^{3+} • • • His-351 $N^{\varepsilon 2}$ = 2.2Å) and oxygen atom of conserved water molecule, W-1 (Fe^{3+} • • • OW-1 = 2.2Å) from the distal heme side. W-1 forms a hydrogen bond with bromide anion (Br^- • • • OW-1 = 3.5Å). It is also hydrogen bonded to His-109 $N^{\varepsilon 2}$ (Br^- • • • His-109 $N^{\varepsilon 2}$ = 2.9Å). The bromide anion in turn is hydrogen bonded to another conserved water molecule W-5′ (Br^- • • • OW-5' = 3.0Å) which is linked to chloride ion (OW-5' • • • Cl^- = 3.2Å) along the channel. The chloride ion is hydrogen bonded to next water molecule, W-7′ (Cl^- • • • OW-7' = 3.2Å). The hydrogen bonded chain involving substrate anions and water molecules is branched at water molecule W-7′ in two directions, one to I^- and

another to SCN^- anions. The hydrogen bonded chain towards I^- includes W-8′ (OW-7' ••• OW-8' = 2.9Å), W-9′ (OW-8' ••• OW-9' = 3.0Å) and I^- (OW-9' ••• I^- = 3.5Å). I^- is further hydrogen bonded to Thr-425 N (I^- ••• Thr-425 N = 3.2Å). In the second branch, W-7′ is hydrogen bonded to nitrogen atom of SCN^- ion (OW-7' ••• N = 2.6Å) whereas the sulfur atom of SCN^- ion is directly hydrogen bonded to Asn-230 (S ••• Asn-230 $N^{\varepsilon 2}$ = 3.2Å) and water molecule W-11′ (S ••• OW-11' = 3.0Å) which in turn is hydrogen bonded to Ser-235 (OW-11' ••• Ser-235 O^{γ} = 2.5Å) and Asn-230 (OW-11' ••• Asn-230 O = 2.6Å). The SCN^- ion is also hydrogen bonded through its N atom to another water molecule W -10' (N ••• OW-10' = 3.2Å) which in turn is hydrogen bonded to Phe-254 (OW-10' ••• Phe-254 O = 2.8Å). Because of these interactions, the conformations of residues Asn-230, Ser-235, Pro-236 and Phe-254 have changed significantly. In the overall arrangement, the outermost position in the channel is occupied by iodide ion while SCN^- is held in a side pocket but both are linearly connected to the heme iron through the hydrogen bonded chains involving W-9′, W-8′, W-7′, Cl^-, W-5′, Br^- and W-1. It may be mentioned here that SCN^- ion has been observed at the same SCN^- ion binding pocket in the complex with SCN^- (PDB ID: 3QL6) as well as at the position of Br^- ion for catalytic conversion (PDB IDs: 3ERH and 3ERI). The position of I^- observed in this structure also appears to be unique as it has been reported in another complex with I^- (PDB ID: 3QL6) and no other halide anion has been observed at this site so far. In order to provide the stabilizing hydrogen bonded interaction to I^- ion in the channel with Thr-425 N, the conformation of Thr-425 is appreciably altered where the Thr-425 containing tetrapeptide Gln-423 - Pro-424 - Thr-425 - His-426 of the channel forming loop 420-433 adopts a type II β-turn conformation (**Figure 4A** (**a**)) unlike its conformation in the absence of iodide ion at this position where the corresponding peptide adopts a highly distorted type I β-turn conformation (**Figure 4A** (**b**)). Similarly the binding of SCN^- ion in the channel induced an appreciable conformational change in the loop, Asn-230 - Pro-236 (**Figure 4B**). The position of chloride ion is located at an appropriate position in the diffusion channel to form a van der Waals contact at a distance of 3.7Å from the side chain of Phe-381 from one side of the channel wall. From the opposite side, the side chain of Phe-254 is flipped towards the diffusion channel with a rotation of χ_1 = -174° from its original away position with χ_1 = -74° and forms a similar van der Waals interaction with the Cl^- ion at a distance of 3.7Å (**Figure 4C**). On further moving towards the heme moiety, the bromide atom is located at a distance of 3.7Å from His-109 $C^{\varepsilon 1}$ while its distance from the position of the corresponding atom observed in the native structure (PDB ID: 3GC1) is more than 4.0Å (**Figure 4D**). Although His-109 is tightly held at its position due to its interactions with conserved water molecule W-1 and also because it belongs to a highly ordered α-helix H2 which is anchored to calcium ion through two linkages through Asp-110. These data clearly indicate that all the three halide ions Br^-, Cl^- and I^- are stabilized at their respective observed positions through induced fit by changing conformations of neighboring residues that included His-109, Phe-254 and Thr-425. In the resting state, these might be favourable positions of the respective halide ions. On the other hand the position of SCN^- ion is unique and seems to be repeatedly occupied by SCN^- ion in LPO (PDB IDs: 3QL6, 3Q9K, 3PY4 and 3OGW).

Nomenclature of subsites in LPO

The ligand diffusion channel and the active site in LPO are designated hereafter as the substrate-binding site. Since the substrate-binding site constitutes a significant region in the protein and provides characteristic interactions at different subsites in the channel, it would be appropriate to divide the substrate-binding site into four subsites. In the reaction mechanism of catalysis, the position of conserved water molecule W-1 has to be eventually occupied by H_2O_2 when the reaction involving heme moiety of lactoperoxidase, H_2O_2 and the substrate produces various useful antimicrobial agents. Therefore, the site of W-1 is considered as the activity center in the protein. In the present structure, the position next to the active center in the substrate-binding site is occupied by Br^- ion which is stabilized by the interactions involving residues, Gln-105, His-109, Arg-255 as well as conserved water molecule W-1. This site is designated as subsite 1 (S1). The next interaction subsite is occupied by Cl^- ion which interacts with Phe-254, Arg-255 and Phe-381 and two water molecules W-5′ and W-7′. This subsite is named as subsite 2 (S2). On further moving away from the heme iron to the next subsite where SCN^- ion is located. SCN^- ion is stabilized by several interac-

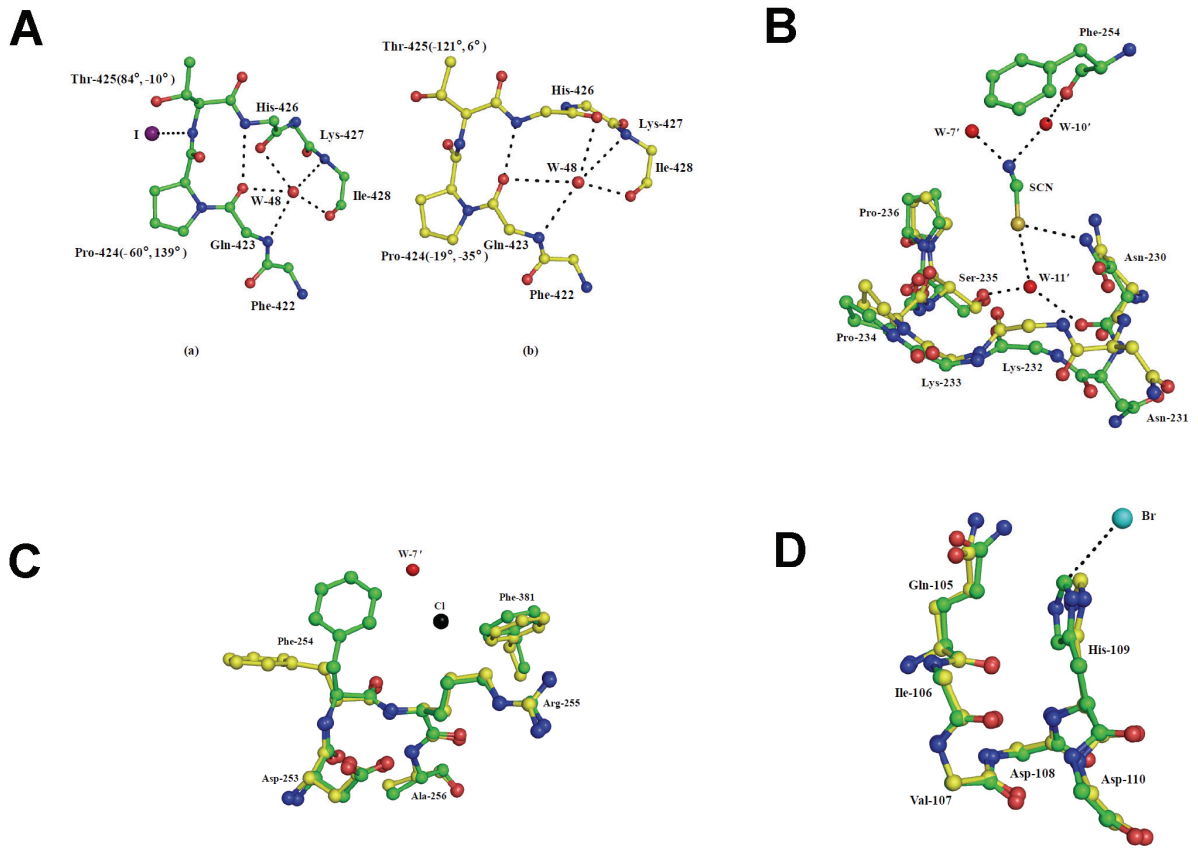

Figure 4. (A) A part of the important loop of subsite 4 showing important conformational differences with (a) bound I- ion and (b) without I- ion. (B) The comparison of the segment consisting of residues that interact with SCN- in subsite 3 (a) bound SCN- ion and (b) without SCN- ion. (C) The differences in conformations at subsite 2 with (a) bound Cl- ion and (b) without Cl- ion. (D) The comparison of structures of subsite 1 (a) with Br- ion and (b) without Br- ion.

tions from residues, Asn-230, Ser-235 and Pro-236 and water molecules W-7′, W-10′ and W-11′. This location is called subsite 3 (S3). The last region in the substrate-binding site is occupied by I- ion which interacts with W-9′, Thr-425, Pro-424, Pro-234 and Phe-239. It is termed as subsite 4 (S4). These four principal subsites are illustrated schematically in **Figure 5**. This classification of the substrate-binding site in lactoperoxidase provides a clear understanding of the stereochemical aspects of enzyme substrate interactions.

Analysis and implications

This is for the first time that four different substrate ions, SCN-, I-, Cl- and Br- were observed simultaneously in the substrate binding site on the distal heme side in heme peroxidases. In this structure, heme iron is coordinated to His-351 $N^{\varepsilon 2}$ on the proximal heme side at a distance of 2.2Å. It coordinates to W-1 on the distal heme side also at a distance of 2.2Å. The three halide ions are linearly located in the substrate diffusion channel which are separated by one or more water molecules. The water molecule W-1 separates the heme iron from Br- ion while W-5′ is positioned between Br- and Cl- ions. The Cl- and I- ions are separated by three water molecules W-7′, W-8′ and W-9′. Similarly, SCN- and Cl- ions are separated by a water molecule, W-7′. According to the locations of four anions in the channel, the position closest to the heme moiety is occupied by bromide ion while the iodide ion is held at the farthest position from the heme iron. The chloride ion is in the middle while SCN- ion is placed in a side pocket. The linear chain of W-1, Br-, W-5′, Cl- and W-7′ bifurcates at W-7′. One chain ends at SCN- ion while the other chain continues to

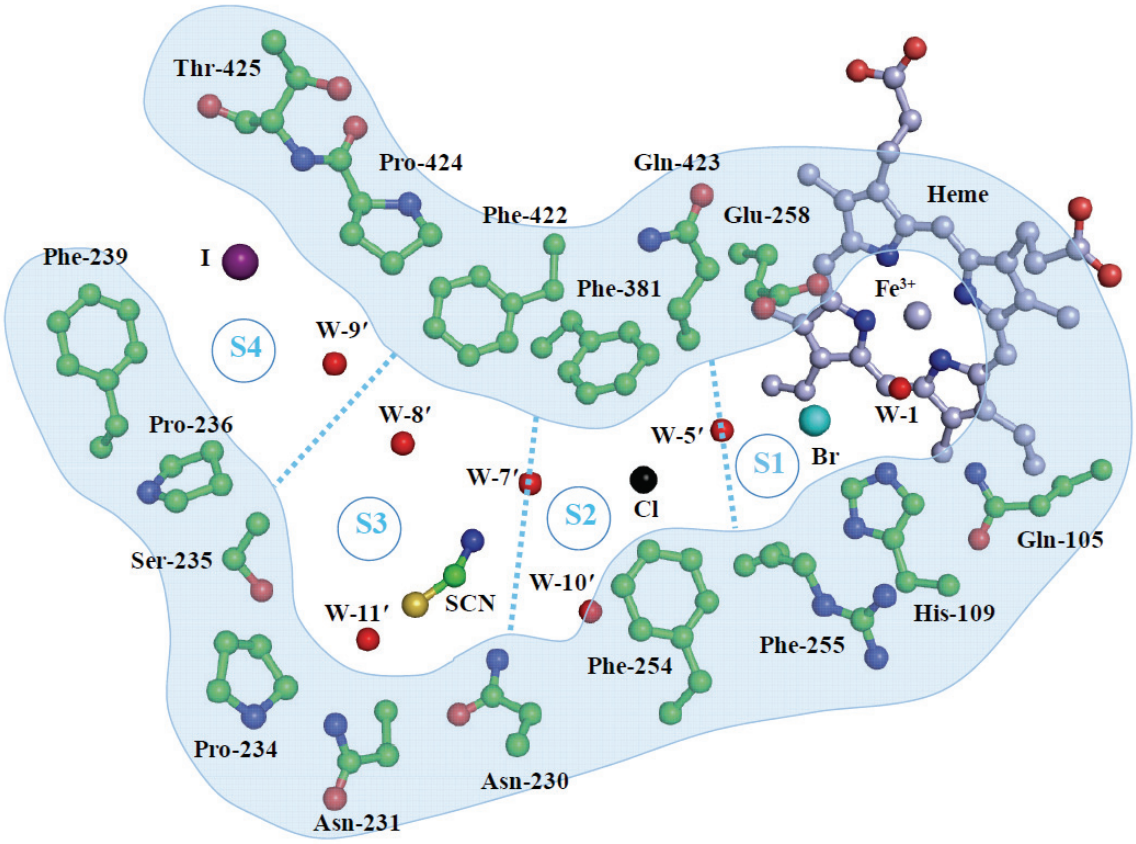

Figure 5. The definition of subsites in the substrate-binding site on the distal heme side as S1, S2, S3 and S4.

W-8′, W-9′ and I^-. The crystallization mixture contained equimolar proportions of all the four ions, SCN^-, I^-, Cl^- and Br^- at a higher molar concentrations than that of protein as well as these crystals were further soaked in the buffer containing all the four anions. Each step was allowed enough time for the anions to diffuse into the binding site in LPO. Under these conditions, it was expected that all the anions would have occupied their positions with full occupancies. Therefore, the anion that occupied the closest position with respect to the heme iron in the substrate-binding site on the distal heme side represented the position of the most preferred substrate ion for LPO. In the present case, the Br^- ion was observed at the closest position indicating that it was the most preferred substrate ion. The Cl^- ion followed it and hence it was second most preferred substrate ion. The third was SCN^- ion which was separated from Cl^- ion by one water molecule, W-7′ whereas I^- ion on the other hand was the last because it was away from Cl^- ion by three water molecules, W-7′, W-8′ and W-9′. These observations indicated the role of a very fine stereochemical preference of the substrate binding site of LPO for the inorganic substrates, I^-, SCN^-, Cl^- and Br^-. These results also imply that all the four inorganic substrates have a full access to the active site in LPO and would possibly get converted into the products. Therefore, all of them are potential substrates for LPO. However, because of equal concentrations of these substrates, it may be inferred from the positions of individual substrate ions that LPO enzyme shows a preference in the order of Br^- > Cl^- > SCN^- > I^-. These are new insights pertaining to the action and preference of LPO for the inorganic substrates, SCN^-, I^-, Br^- and Cl^-. This also clarifies the notion that SCN^- is not the only inorganic substrate for LPO.

Acknowledgements

The authors acknowledge the financial grant from the Department of Science and Technology (DST) of the Ministry of Science and Technology

New Delhi. MS thank the Council of Scientific and Industrial Research (CSIR), New Delhi for the award of fellowships. NP thanks the Indian Council of Medical Research (ICMR), New Delhi for the award of fellowship. TPS thanks Department of Biotechnology (DBT), Ministry of Science and Technology, New Delhi for the award of Distinguished Biotechnology Research Professorship to him.

Address correspondence to: Dr. Singh TP, Department of Biophysics, All India Institute of Medical Sciences, Ansari Nagar, New Delhi – 110 029, India Tel: +91-11-2658-8931; Fax: +91-11-2658-8663; E-mail: tpsingh.aiims@gmail.com

References

[1] Zhang H, Dunford HB. Hammett pδ correlation for reactions of lactoperoxidase compound II with phenols. Can J Chem 1993; 71: 1990-1994.

[2] Monzani E, Gatti AL, Profumo A, Casella L and Gullotti M. Oxidation of phenolic compounds by lactoperoxidase. Evidence for the presence of a low-potential compound II during catalytic turnover. Biochemistry 1997; 36: 1918-1926.

[3] Metodiewa D, Reszka K and Dunford HB. Oxidation of the substituted catechols dihydroxyphenylalanine methyl ester and trihydroxyphenylalanine by lactoperoxidase and its compounds. Arch Biochem Biophys 1989; 274: 601-608.

[4] Metodiewa D, Reszka K and Dunford HB. Evidence for a peroxidatic oxidation of norepinephrine, a catecholamine, by lactoperoxidase. Biochem Biophys Res Commun 1989; 160: 1183-1188.

[5] Ferrari RP, Laurenti E, Casella L and Poli S. Oxidation of catechols and catecholamines by horseradish-peroxidase and lactoperoxidase: ESR spin stabilization approach combined with optical methods. Spectrochim Acta 1993; 49: 1261-1267.

[6] Doerge DR, Decker CJ. Inhibition of peroxidase-catalyzed reactions by arylamines: mechanism for the anti-thyroid action of sulfamethazine. Chem Res Toxicol 1994; 7: 164-169.

[7] Oakley GG, Devanaboyina U, Robertson LW and Gupta RC. Oxidative DNA damage induced by activation of polychlorinated biphenyls (PCBs): implications for PCB-induced oxidative stress in breast cancer. Chem Res Toxicol 1996; 9: 1285-1292.

[8] Sipe HJ, Jr Jordan SJ, Hanna PM and Mason RP. The metabolism of 17 beta-estradiol by lactoperoxidase: a possible source of oxidative stress in breast cancer. Carcinogenesis 1994, 15: 2637-2643.

[9] Cavalieri EL, Stack DE, Devanesan PD, Todorovic R, Dwivedy I, Higginbotham S, Johansson SL, Patil KD, Gross ML, Gooden JK, Ramanathan R, Cerny RL and Rogan EG. Molecular origin of cancer: catechol estrogen-3,4-quinones as endogenous tumor initiators. Proc Natl Acad Sci USA 1997; 94: 10937-10942.

[10] Ghibaudi EM, Laurenti E, Beltramo P and Ferrari RP. Can estrogenic radicals, generated by lactoperoxidase, be involved in the molecular mechanism of breast carcinogenesis? Redox Rep 2000; 5: 229-235.

[11] RamaKrishna NV, Li KM, Rogan EG, Cavalieri EL, George M, Cerny RL and Gross ML. Adducts of 6-methylbenzo[a]pyrene and 6-fluorobenzo [a]pyrene formed by electrochemical oxidation in the presence of deoxyribonucleosides. Chem Res Toxicol 1993; 6: 837-845.

[12] Zeng J, Fenna RE. X-ray crystal structure of canine myeloperoxidase at 3Å resolution. J Mol Biol 1992; 226: 185-207.

[13] Davey CA, Fenna RE. 2.3Å resolution X-ray crystal structure of the bisubstrate analogue inhibitor salicylhydroxamic acid bound to human myeloperoxidase: a model for a prereaction complex with hydrogen peroxide. Biochemistry 1996, 35: 10967-10973.

[14] Fiedler TJ, Davey CA and Fenna RE. X-ray crystal structure and characterization of halide-binding sites of human myeloperoxidase at 1.8Å resolution. J Biol Chem 2000; 275: 11964-11971.

[15] Blair-Johnson M, Fiedler T and Fenna R. Human myeloperoxidase: structure of a cyanide complex and its interaction with bromide and thiocyanate substrates at 1.9Å resolution. Biochemistry 2001; 40: 13990-13997.

[16] Singh AK, Singh N, Sharma S, Singh SB, Kaur, P, Bhushan A, Srinivasan A and Singh TP. Crystal structure of lactoperoxidase at 2.4Å resolution. J Mol Biol 2008; 376: 1060-1075.

[17] Singh AK, Singh N, Sharma S, Shin K, Takase M, Kaur P, Srinivasan A and Singh TP. Inhibition of lactoperoxidase by its own catalytic product: crystal structure of the hypothiocyanate-inhibited bovine lactoperoxidase at 2.3Å resolution. Biophys J 2009; 96: 646-654.

[18] Sheikh IA, Singh AK, Singh N, Sinha M, Singh SB, Bhushan A, Kaur P, Srinivasan A, Sharma S and Singh TP. Structural evidence of substrate specificity in mammalian peroxidases: structure of the thiocyanate complex with lactoperoxidase and its interactions at 2.4Å resolution. J Biol Chem 2009; 284: 14849-14856.

[19] Singh AK, Singh N, Sinha M, Bhushan A, Kaur P, Srinivasan A, Sharma S and Singh TP. Binding modes of aromatic ligands to mammalian heme peroxidases with associated functional implications: crystal structures of lactoperoxidase complexes with acetylsalicylic acid, salicylhydroxamic acid, and benzylhydroxamic acid. J Biol Chem 2009; 284: 20311-20318.

[20] Singh AK, Kumar RP, Pandey N, Singh N, Sinha M, Bhushan A, Kaur P, Sharma S and Singh TP.

Mode of binding of the tuberculosis prodrug isoniazid to heme peroxidases: binding studies and crystal structure of bovine lactoperoxidase with isoniazid at 2.7Å resolution. J Biol Chem 2010; 285: 1569-1576.
[21] Singh AK, Singh N, Tiwari A, Sinha M, Kushwaha GS, Kaur P, Srinivasan, A, Sharma S and Singh TP. First structural evidence for the mode of diffusion of aromatic ligands and ligand-induced closure of the hydrophobic channel in heme peroxidases. J Biol Inorg Chem 2010; 15: 1099-1107.
[22] Ferrari RP, Ghibaudi EM, Traversa S, Laurenti E, De Gioia L and Salmona M. Spectroscopic and binding studies on the interaction of inorganic anions with lactoperoxidase. J Inorg Biochem 1997; 68: 17-26.
[23] Harrison JE, Schultz J. Studies on the chlorinating activity of myeloperoxidase. J Biol Chem 1976; 251: 1371-1374.
[24] van Dalen CJ, Kettle AJ. Substrates and products of eosinophil peroxidase. Biochem J 2001; 358: 233-239.
[25] Kimura S, Kotani T, McBride OW, Umeki K, Hirai K, Nakayama T and Ohtaki S. Human thyroid peroxidase: complete cDNA and protein sequence, chromosome mapping, and identification of two alternately spliced mRNAs. Proc Natl Acad Sci USA 1987; 84: 5555-5559.
[26] Shindler JS, Bardsley WG. Steady-state kinetics of lactoperoxidase with ABTS as chromogen. Biochem Biophys Res Commun 1975; 67: 1307-1312.
[27] Otwinowski Z, Minor W. Processing of X-ray Diffraction Data Collected in Oscillation Mode. Methods in Enzymology 1997; 276: 307-326.
[28] Brunger AT, Adams PD, Clore GM, DeLano WL, Gros P, Grosse-Kunstleve RW, Jiang JS, Kuszewski J, Nilges M, Pannu NS, Read RJ, Rice LM, Simonson T and Warren GL. Crystallography & NMR system: A new software suite for macromolecular structure determination. Acta Crystallogr 1998; D54: 905-921.
[29] Jones TA, Zou JY, Cowan SW and Kjeldgaard M. Improved methods for building protein models in electron density maps and the location of errors in these models. Acta Crystallogr 1991; A47: 110-119.
[30] Laskowski RA, Macarthur M, Moss D and Thornton J. PROCHECK: a program to check stereo chemical quality of protein structures. J Appl Crystallogr 1993; 26: 283-290.
[31] Ramachandran GN, Sasisekaran V. Conformation of polypeptides and proteins. Adv Protein Chem 1968; 23: 283-438.
[32] Davis IW, Leaver-Fay A, Chen VB, Block JN, Kapral GJ, Wang X, Murray LW, Arendall WB 3rd, Snoeyink J, Richardson JS and Richardson DC. MolProbity: all-atom contacts and structure validation for proteins and nucleic acids. Nucleic Acids Res 2007; 35: W375-383.
[33] DeLano WL. The PyMol molecular Graphics System, DeLano Scientific, San Carlos CA. 2002; http://www.pymol.org.